Nano Res. 2010, 3(12): 895–901
DOI 10.1007/s12274-010-0063-z
Research Article

ISSN 1998-0124
CN 11-5974/O4

A Facile Method to Improve the High Rate Capability of Co_3O_4 Nanowire Array Electrodes

Hua Cheng[1,2], Zhou Guang Lu[1,2], Jian Qiu Deng[1], C. Y. Chung[1], Kaili Zhang[3], and Yang Yang Li[1] (✉)

[1] Department of Physics and Materials Science, City University of Hong Kong, HKSAR, China
[2] School of Chemistry and Chemical Engineering, Central South University, Changsha, Hunan 410083, China
[3] Department of Manufacturing Engineering and Engineering Management, City University of Hong Kong, HKSAR, China

Received: 6 September 2010 / Revised: 16 October 2010 / Accepted: 20 October 2010

ABSTRACT

The capability of fast charge and fast discharge is highly desirable for the electrode materials used in supercapacitors and lithium ion batteries. In this article, we report a simple strategy to considerably improve the high rate capability of Co_3O_4 nanowire array electrodes by uniformly loading Ag nanoparticles onto the surfaces of the Co_3O_4 nanowires via the silver-mirror reaction. The highly electrically conductive silver nanoparticles function as a network for the facile transport of electrons between the current collectors (Ti substrates) and the Co_3O_4 active materials. High capacity as well as remarkable rate capability has been achieved through this simple approach. Such novel Co_3O_4–Ag composite nanowire array electrodes have great potential for practical applications in pseudo-type supercapacitors as well as in lithium ion batteries.

KEYWORDS

Cobalt oxide (Co_3O_4), nanowire arrays, electrode materials, supercapacitors, lithium ion batteries, high rate capability

1. Introduction

Successful utilization of sustainable energy resources, such as solar, water, or wind, largely relies on the development of efficient electrical energy storage and conversion (EESC) devices. Lithium ion batteries (LIBs) and supercapacitors (SCs) are at the forefront of R&D on EESC devices [1]. They have been extensively considered as power sources for electric vehicles (EVs), portable electronics such as cell phones, cameras, laptop computers and pulsed lasers, and large power backup for the electric grid [2, 3]. For both LIBs and SCs, a critical challenge is to develop electrodes possessing high energy density and power uptake capability, i.e., the ability to deliver a large amount of charge in a very short time [4].

Co_3O_4 has been demonstrated to be a promising electrode material for LIBs and pseudo-type SCs due to its low environmental footprint, low cost and extremely high theoretical specific capacitance (3560 F/g) for SCs and capacity (890 mA·h/g) for LIBs [5–22]. Furthermore, cobalt oxide directly grown on current collectors in the form of highly oriented nanowires (NWs) has several additional advantages for applications in electrodes [2]. First, the as-grown NWs have good mechanical contact with the current

Address correspondence to yangli@cityu.edu.hk

collectors, being free of the binders and carbon conductors that are generally used in making conventional electrodes, which helps increase the specific energy density [23, 24]. Second, the NW array structure can expand the electroactive area for pseudocapacitive reactions, provide effective electrolyte-accessible channels for ion transportation, and shorten the distance for ion diffusion, leading to considerably reduced internal resistance and substantially improved power performances [25]. Third, the geometry of such novel NW arrays is believed to help accommodate strain arising from the electrochemical redox reactions as well as the large volume expansion during the Li^+ insertion and de-insertion [26]. Therefore, Co_3O_4 NW array electrodes are an attractive candidate for the construction of next-generation ultrahigh performance LIBs and SCs [7].

Wu et al. have successfully prepared mesoporous Co_3O_4 NW arrays on Ti substrates by a template-free ammonia-evaporation-induced method [24] and employed them as anodes for constructing LIBs. They achieved a reversible capacity of >700 mA·h/g at a current of 1 C and >350 mA·h/g at 50 C [23]. Gao et al. have demonstrated that a specific capacitance of 746 F/g at a current density of 5 mA/cm^2 can be obtained from supercapacitors derived from Co_3O_4 NW arrays [25]. In this article we show that both energy density and rate performance of Co_3O_4 NW array electrodes can be substantially enhanced through the incorporation of highly conductive silver nanoparticles onto the surfaces of the Co_3O_4 NWs.

2. Experimental

2.1 Preparation of Co_3O_4 NW arrays on Ti substrates

The experimental procedure for the synthesis of Co_3O_4 NW arrays on Ti substrates was the same as described in Refs. [23, 27]. In a typical procedure, 15 mmol of $Co(NO_3)_2$ was dissolved in 15 mL of deionized (DI) water. Then 60 mL of 25% ammonia solution was added dropwise to the Co^{2+} solution within 5 min with vigorous stirring. Before being transferred into a covered Petri dish, the above solution was stirred for another 10 min. Meanwhile, one side of a cleaned Ti wafer was covered by a layer of nail polish. The Ti wafer was put into the Petri dish with the other side facing downwards, being about 2–3 mm away from the bottom of the dish. The reaction setup was then kept in an oven at 90 ℃ for 14 h.

2.2 Preparation of Ag–Co_3O_4 composite NW arrays

The conventional silver-mirror reaction was utilized to deposit Ag nanoparticles onto the surfaces of the Co_3O_4 NW arrays. Typically, 0.01 mol of $AgNO_3$ powder was dissolved in 50 mL DI water at room temperature to prepare a clear solution and then 50 mL of 0.2 mol/L NaOH solution was added to the $AgNO_3$ solution giving a brown precipitate. Concentrated (10 mol/L) ammonia solution was then added dropwise into the mixed solution under vigorous stirring until the brown precipitate just dissolved. 50 mL of 0.4 mol/L glucose solution was then added to the mixture with vigorous stirring. The beaker was transferred to a water bath at 90 ℃. Ag coating of the Ti/Co_3O_4 NW array electrode was carried out by repeating the following procedure 6 times: (1) immersion into the heated $AgNO_3$–glucose solution for 5 min, (2) washing with DI water, ethanol and finally acetone, and (3) drying in a vacuum oven at 60 ℃ for 2 h.

2.3 Materials characterizations

X-ray diffraction (XRD) patterns were collected on a Philips powder diffractometer using Cu Kα radiation (λ = 1.5405 Å). Sample morphologies were examined with a scanning electron microscope (JEOL-820) and transmission electron microscope (Philips CM-20). Elemental mappings were conducted using an energy-dispersive X-ray (EDX) device attached to a JEOL-6490 SEM. For the elemental mapping and TEM, the Co_3O_4 NWs were scratched from the Ti substrate and re-dispersed in ethanol solution by ultrasonification and then dropped onto the surface of silicon wafers. No metal coating treatment was performed on the samples before characterization by electron microscopy.

2.4 Electrochemical performance evaluation

The Co_3O_4 NW arrays grown on Ti foils were directly used as electrodes for electrochemical characterization. Coin cells (2025) for LIBs were assembled in an argon-filled glove-box with Li metal foil (Aldrich, USA) as

the counter and reference electrode, one layer of Celgard 2025 (Celgard, Inc., USA) as the separator, and $LiPF_6$ (1 mol/L) dissolved in an ethylene carbonate (EC)/dimethyl carbonate (DMC) mixture (1/1 *w*/*w*) as the electrolyte. Galvanostatic electrochemical experiments were carried out on an Arbin Instruments (BT 2000, College Station, Texas, USA) battery cycler at room temperature. The traditional three-electrode cells were assembled for SC characterization employing the Ti–Co_3O_4 NW arrays as the working electrode, a Pt foil (2 cm × 5 cm × 0.005 cm) as the counter electrode and a saturated calomel electrode (SCE) as the reference electrode, and a 1 mol/L aqueous KOH solution as the electrolyte. The measurements were performed on a Princeton Applied Research (PAR) V3 instrument. To determine the mass of the Co_3O_4–Ag active materials (m_a) in the electrodes, we measured the original weight (m_0) of the Ti substrate with the grown Co_3O_4–Ag NW arrays, before any electrochemical testing. After testing, the Co_3O_4–Ag NW active materials were scratched off the Ti substrate by strong ultrasonification and then the net weight of the Ti substrate (m_s) was measured. The mass of the Co_3O_4–Ag active materials is given by $m_a = m_0 - m_s$. The specific discharge capacitance (C_m) of the capacitors can be calculated as follows: $C_m = I\Delta t/(m_a\Delta V)$, where I is the discharge current, Δt is the duration required for discharging to a cut-off voltage of −0.4 V, m_a is the mass of active material in the working electrode, and ΔV is the cut-off potential difference between charge and discharge, i.e., 0.8 V in the these experiments.

3. Results and discussion

3.1 XRD

Figure 1 shows the XRD pattern of the cobalt oxide NW arrays (a) before and (b) after Ag incorporation. Besides the reflections arising from the Ti substrate, the patterns of the samples before and after Ag coating can both be indexed to spinel Co_3O_4. This suggests that the NW arrays prepared by the template-free ammonia-evaporation-induced method are mainly composed of spinel Co_3O_4, which is in good agreement with previous reports [23–25]. Moreover, the Ag coating process did not alter the crystal phase of the Co_3O_4 NW arrays.

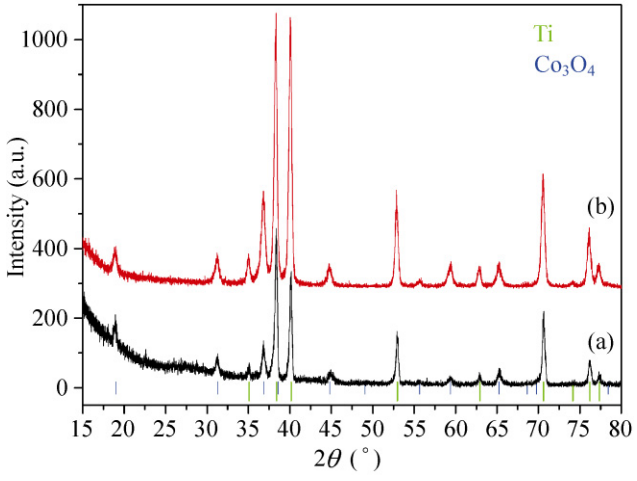

Figure 1 XRD patterns of the cobalt oxide NW arrays (a) before and (b) after Ag coating. The inset bottom green and blue bars indicate the standard reflections from Ti (JCPDS-659622) and Co_3O_4 (JCPDS-431003), respectively

3.2 Electron microscopy and elemental mapping

The SEM images in Figs. 2(a) and 2(b) reveal that Co_3O_4 NWs with diameters of 400–900 nm and lengths ranging from 10 to 15 μm were formed as arrays on the Ti substrate. The very sharp image observed in Fig. 2(b) is due to electron charging resulting from the low electronic conductivity of the pristine Co_3O_4 NWs. TEM indicates that the NWs are quasi-single-crystal in nature (Fig. 2(d)) and resemble a tubular structure with a mesoporous cavity running throughout the wire center (Fig. 2(e)), which is consistent with previous reports [23, 24, 28]. After incorporation of the highly conductive silver, the SEM image (Fig. 2(c)) is much clearer than the one without Ag incorporation (Fig. 2(b)), which can be attributed to the enhancement in electronic conductivity resulting from the Ag coating on the surface of Co_3O_4 NWs. Some Ag nanoparticles are observable on the surface of the Co_3O_4 NWs as indicated by red arrows in the TEM image (Fig. 2(e)). Figure 3 shows the EDX spectrum and the corresponding Co Kα1 and Ag Lα1 elemental mappings of two selected Co_3O_4–Ag NWs that have been scratched off the Ti substrate and re-dispersed onto a Si wafer. From the EDX result (Fig. 2(b)), the content of Ag in the as-prepared Co_3O_4–Ag composite NWs is about 3 wt%. It is evident from Figs. 3(c) and 3(d) that the Ag nanoparticles are homogeneously distributed over the surfaces of the Co_3O_4 NWs.

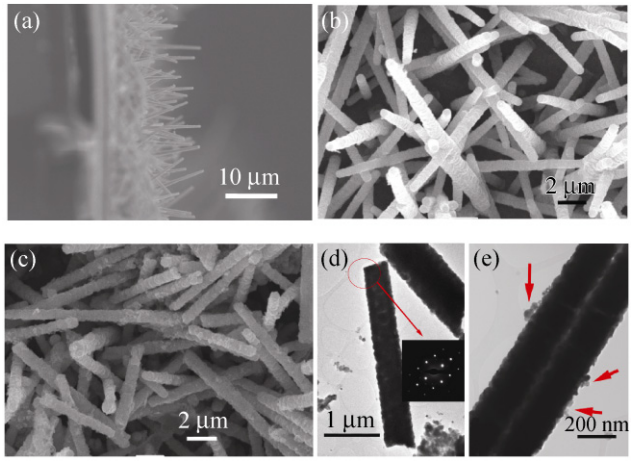

Figure 2 (a) Cross-sectional SEM, (b, c) plan-view SEM, and (d, e) TEM images of the Co_3O_4 NW arrays before (a, b, d) and after (c, e) coating with Ag. The electron diffraction pattern of the Co_3O_4 NWs before Ag coating is shown in the inset of (d)

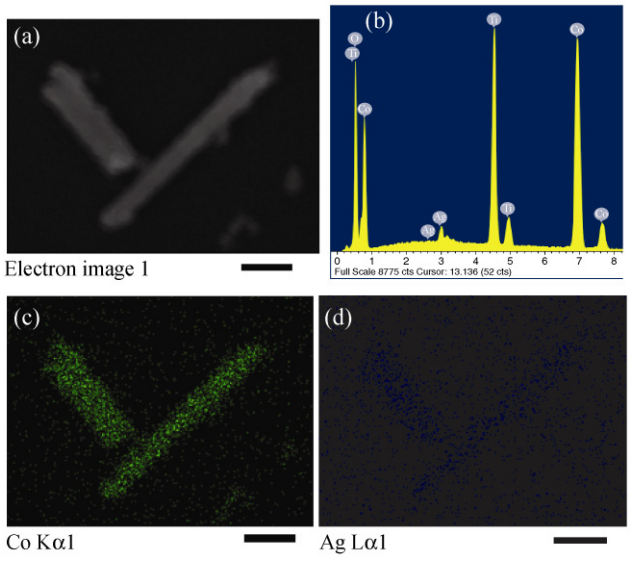

Figure 3 (a) SEM image and (b) the corresponding EDX spectrum of two selected Co_3O_4–Ag NWs that have been scratched off the Ti substrate and re-dispersed onto a Si wafer. The corresponding elemental distributions of (c) Co Kα1 and (d) Ag Lα1 in the two selected Co_3O_4–AgNWs. The scale bar represents 1 μm

3.3 Supercapacitors

Figure 4(a) shows galvanostatic charge and discharge curves of the Co_3O_4 NW array electrodes, before and after Ag incorporation, at various current densities. The reversible specific discharge capacitances of the pristine Co_3O_4 NW arrays were calculated to be 922, 768, and 516 F/g at current densities of 2, 5, and 10 A/g, respectively. Compared with the pristine Co_3O_4 NW arrays, the Co_3O_4–Ag NW array electrode displays better capacitive performances with higher specific capacitances of 1006, 950, and 900 F/g at current densities of 2, 5, and 10 A/g, respectively. The benefit of incorporating highly conductive Ag can be further substantiated by considering the capacitive properties at high current density. For the pristine Co_3O_4 NW arrays, the capacitance retention at 5 and 10 A/g was found to be 83.3% and 54.2% of that at 2 A/g, respectively. After being coated with Ag, however, the NW array electrode retained more than 95% (at 5 A/g) and 90% (at 10 A/g) of the capacitance at the low current density of 2 A/g. Figure 4(b) shows the specific discharge capacitance as a function of cycle number at a

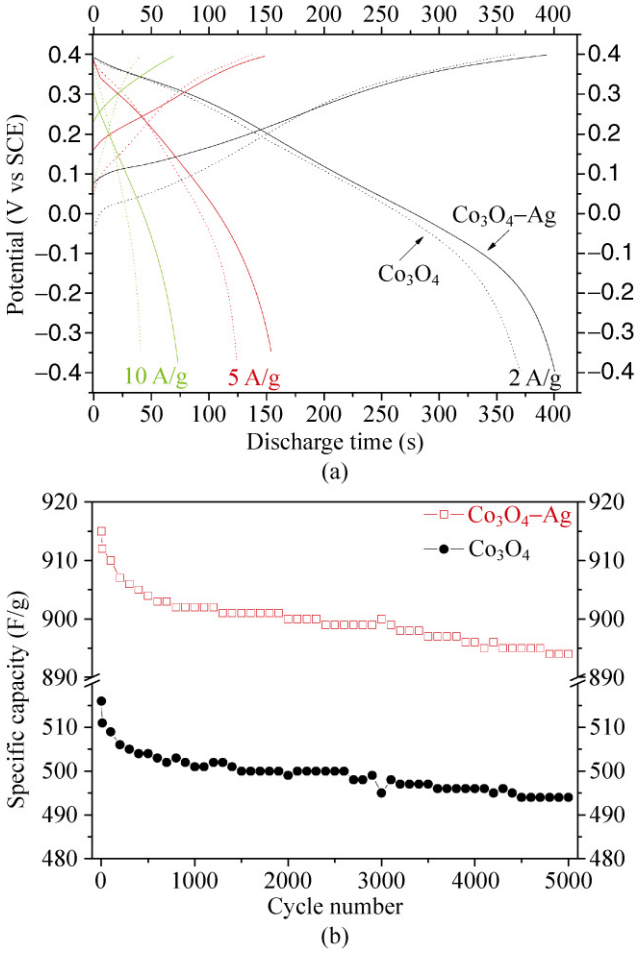

Figure 4 Capacitive performances of the Co_3O_4 NW arrays electrodes with, and without, Ag incorporation: (a) galvanostatic charge and discharge curves at various current densities; (b) specific discharge capacitance versus cycle number at a current density of 10 A/g

current density of 10 A/g for the Ag-incorporated Co_3O_4 NW array electrodes and the pristine Co_3O_4 NW arrays electrodes. For both types of electrodes, the value of the capacitance continuously decreases over the first 100 cycles and becomes stable in subsequent cycles. The capacitance retention is more than 95% of the initial value after 5000 cycles for both types of electrodes. It is evident that the Ag-incorporated Co_3O_4 NW array electrodes have much higher capacitance than their pristine counterpart at high current density. The results in Fig. 4 clearly demonstrate that the incorporation of highly conductive Ag improves the performance of the Co_3O_4 active materials and, most importantly, substantially enhances the power capability of the Co_3O_4 NW array electrodes.

3.4 Lithium ion batteries

Figure 5(a) shows the stabilized electrochemical voltage profiles of the Co_3O_4 NW array electrodes with and without Ag incorporation at a very low rate (100 mA/g). It is clear that the Co_3O_4–Ag electrode has slightly lower electrochemical charge and discharge potential and higher reversible capacity (~1050 mA·h/g) compared with the pristine Co_3O_4 electrode (~975 mA·h/g). The lower electrochemical potential implies that the actual LIBs assembled from our Co_3O_4–Ag NW arrays as an anode coupled with a cathode (for example $LiCoO_2$) would have higher working potential, leading to improved energy density.

Figure 5(b) shows the specific charge capacity of the Co_3O_4 NW array electrodes as a function of cycle number and current density. It is evident that the Co_3O_4–Ag electrode displays better electrochemical activity than that of the pristine Co_3O_4 electrode. In particular, the rate capability was considerably improved after coating with Ag nanoparticles. The Co_3O_4–Ag electrode showed more than 82% and 45% capacity retention after the current density was increased from 100 to 2000 and 20 000 mA/g, respectively, whereas for the pristine Co_3O_4 electrode, only 74% and 26% of the original capacity was maintained when raising the current density from 100 to 2000 and 20 000 mA/g, respectively. The results in Fig. 5 further confirm the advantages of incorporating highly conductive silver in terms of improving the rate capability of the Co_3O_4 NW array electrodes.

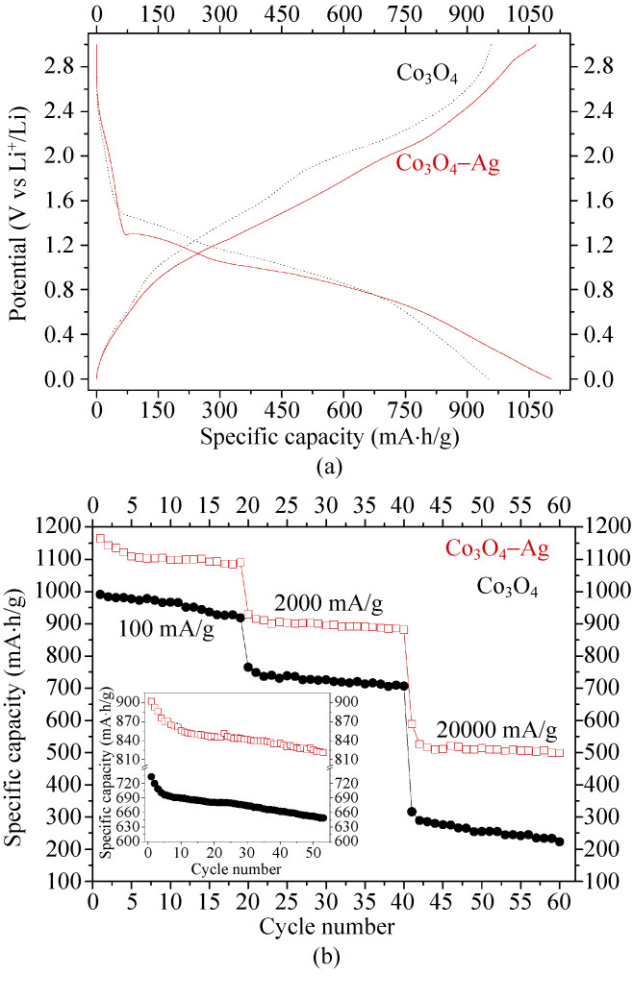

Figure 5 Lithium ion battery performances of the Co_3O_4 NW array electrodes with and without Ag incorporation. (a) The 6th cycle galvanostatic charge and discharge voltage profiles cycled between 3 and 0.005 V at a current density of 100 mA/g. (b) Comparison of the cycling performance of the Co_3O_4 NW array electrodes with and without Ag incorporation under different current rates. The lower-left inset graph in (b) shows the charge capacity as a function of the cycle number of the same electrodes after being tested at 20 000 mA/g for 20 cycles and the current density being reset at 2000 mA/g

After high-rate testing at 20 000 mA/g for 20 cycles, the current density was reduced to 2000 mA/g and the electrodes were further subjected to continuous cycling. The results are shown in the lower-left inset curves of Fig. 5(b). For the Co_3O_4 NW array electrodes with and without Ag incorporation, the specific charge capacities almost recovered their original values of about 900 and 720 mA·h/g, respectively, at a current density of 2000 mAh/g. Although the capacity continuously decreased as the charge-discharge operation

proceeded, the capacity retained more than 91% and 88% of the original values for the electrode with and without Ag incorporation, respectively. This shows that both electrodes demonstrate good reversibility, and compare favorably with conventional nanopowder samples [5]. Moreover, the electrode with an Ag coating is slightly more durable than the one without such a coating.

3.5 Mechanism of the rate capability enhancement

It is generally considered that the electrochemical redox reaction in electrodes occurs only at three-phase boundaries where the active material, the electrolyte, and the current collector meet [29]. As schematically illustrated in Fig. 6, the resistance to electron conduction from the Ti substrates to the Co_3O_4 active materials is very high, due to the inherent low electronic conductivity of Co_3O_4 [23]. However, the deposited Ag network facilitates fast electron transport between the current collectors and the active materials. Furthermore, the Ag coating can revive some dead areas that have become inactive due to their loss of, or very poor, contact with the current collectors, making them electrochemically active, leading to improved utilization of the active materials. Therefore, the very special combination of the mesoporous NW array geometries and the highly electronically conductive Ag coating gives the Co_3O_4 NW array electrodes a very high energy density as well as a remarkable high rate capability.

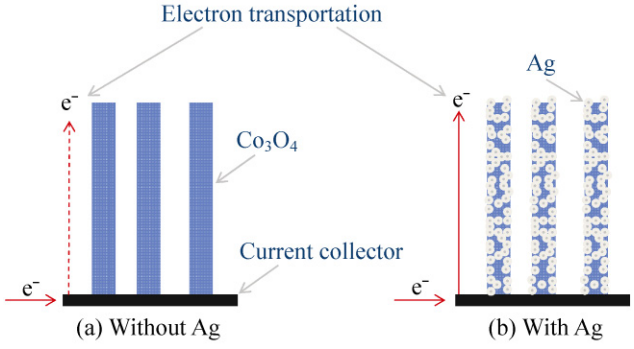

Figure 6 Schematic illustration of the fast electron transportation between the current collectors and the active Co_3O_4 NW arrays through the highly conductive Ag coating. The red solid-line arrow in (b) indicates a much higher conductivity than the red broken-line arrow in (a)

4. Conclusions

A small portion (~3 wt%) of Ag nanoparticles can be homogeneously deposited onto the surfaces of Co_3O_4 NWs by a conventional silver-mirror reaction in order to improve their electronic conductivity. The Ag-coated Co_3O_4 NW arrays can be directly employed as electrodes for half-cell pseudo-type supercapacitors and lithium ion batteries and showed improved specific capacity and markedly enhanced rate capability, which is ascribed to the much improved electronic conductivity resulting from the deposited Ag network.

Acknowledgements

This work was jointly supported by the City University of Hong Kong (Project 7002465). Z. G. L. would like to acknowledge support from the National Natural Science Foundation of China (No. 21001117/B0107).

References

[1] Goodenough, J. B.; Abruña, H. D.; Buchanan, M. V. Basic Research Needs for Electrical Energy Storage: Report of the Basic Energy Sciences Workshop on Electrical Energy Storage [Online], 2007 Apr 04. US Department of Energy. http://www.sc.doe.gov/bes/reports/abstracts.html#EES2007 (accessed September 6, 2010).

[2] Simon, P.; Gogotsi, Y. Materials for electrochemical capacitors. *Nat. Mater.* **2008**, *7*, 845–854.

[3] Armand, M.; Tarascon, J. M. Building better batteries. *Nature* **2008**, *451*, 652–657.

[4] Arico, A. S.; Bruce, P.; Scrosati, B.; Tarascon, J. M.; van Schalkwijk, W. Nanostructured materials for advanced energy conversion and storage devices. *Nat. Mater.* **2005**, *4*, 366–377.

[5] Poizot, P.; Laruelle, S.; Grugeon, S.; Dupont, L.; Tarascon, J. M. Nano-sized transition-metal oxides as negative-electrode materials for lithium-ion batteries. *Nature* **2000**, *407*, 496–499.

[6] Zheng, M. B.; Cao, J.; Liao, S. T.; Liu, J. S.; Chen, H. Q.; Zhao, Y.; Dai, W. J.; Ji, G. B.; Cao, J. M.; Tao, J. Preparation of mesoporous Co_3O_4 nanoparticles via solid–liquid route

and effects of calcination temperature and textural parameters on their electrochemical capacitive behaviors. *J. Phys. Chem. C* **2009**, *113*, 3887–3894.

[7] Nam, K. T.; Kim, D.W.; Yoo, P. J.; Chiang, C.Y.; Meethong, N.; Hammond, P. T.; Chiang, Y. M.; Belcher, A. M. Virus-enabled synthesis and assembly of nanowires for lithium ion battery electrodes. *Science* **2006**, *312*, 885–888.

[8] Kim, H. K.; Seong, T. Y.; Lim, J. H.; Cho, W. I.; Yoon,Y. S. Electrochemical and structural properties of radio frequency sputtered cobalt oxide electrodes for thin-film supercapacitors. *J. Power Sources* **2001**, *102*, 167–171.

[9] Deng, M. J.; Huang, F. L.; Sun, I. W.; Tsai, W. T.; Chang, J. K. An entirely electrocemical preparation of a nano-structured cobalt oxide electrode with superior redox activity. *Nanotechnology* **2009**, *20*, 175602.

[10] Wu, Z. S.; Ren, W. C.; Wen, L.; Gao, L. B.; Zhao, J. P.; Chen, Z. P.; Zhou, G. M.; Li, F.; Cheng, H. M. Graphene anchored with Co_3O_4 nanoparticles as anode of lithium ion batteries with enhanced reversible capacity and cyclic performance. *ACS Nano* **2010**, *4*, 3187–3194.

[11] Kong, L. B.; Lang, J. W.; Liu, M.; Luo, Y. C.; Kang, L. Facile approach to prepare loose-packed cobalt hydroxide nano-flakes materials for electrochemical capacitors. *J. Power Sources* **2009**, *194*, 1194–1201.

[12] Ahn, H. J.; Seong, T. Y. Effect of Pt nanostructures on the electrochemical properties of Co_3O_4 electrodes for micro-electrochemical capacitors. *J. Alloy. Comp.* **2009**, *478*, L8–L11.

[13] Wang, X.; Wu, X. L.; Guo, Y. G.; Zhong, Y. T.; Cao, X. Q.; Ma, Y.; Yao, J. N. Synthesis and lithium storage properties of Co_3O_4 nanosheet-assembled multishelled hollow spheres. *Adv. Funct. Mater.* **2010**, *20*, 1680–1686.

[14] Liu, J.; Xia, H.; Lu, L.; Xue, D. F. Anisotropic Co_3O_4 porous nanocapsules toward high-capacity Li-ion batteries. *J. Mater. Chem.* **2010**, *20*, 1506–1510.

[15] Guo, B.; Li, C. S.; Yuan, Z. Y. Nanostructured Co_3O_4 materials: Synthesis, characterization, and electrochemical behaviors as anode reactants in rechargeable lithium ion batteries. *J. Phys. Chem. C* **2010**, *114*, 12805–12817.

[16] Lu, Y.; Wang, Y.; Zou, Y. Q.; Jiao, Z.; Zhao, B.; He, Y. Q.; Wu, M. H. Macroporous Co_3O_4 platelets with excellent rate capability as anodes for lithium ion batteries. *Electrochem. Commun.* **2010**, *12*, 101–105.

[17] Tian, L.; Zou, H. L.; Fu, J. X.; Yang, X. F.; Wang, Y.; Guo, H. L.; Fu, X. H.; Liang, C. L.; Wu, M. M.; Shen, P. K.; Gao, Q. M. Topotactic conversion route to mesoporous quasi-single-crystalline Co_3O_4 nanobelts with optimizable electrochemical performance. *Adv. Funct. Mater.* **2010**, *20*, 617–623.

[18] Wang, Y.; Xia, H.; Lu, L.; Lin, J. Y. Excellent performance in lithium-ion battery anodes: Rational synthesis of $Co(CO_3)_{0.5}(OH)_{0.11}H_2O$ nanobelt array and its conversion into mesoporous and single-crystal Co_3O_4. *ACS Nano* **2010**, *4*, 1425–1432.

[19] Wang, Y.; Zhang, H. J.; Lu, L.; Stubbs, L. P.; Wong, C. C; Lin, J. Y. Designed functional systems from peapod-like Co@carbon to Co_3O_4@carbon nanocomposites. *ACS Nano* **2010**, *4*, 4753–4761.

[20] Lou, X. W.; Deng, D.; Lee, J. Y.; Archer, L. A. Thermal formation of mesoporous single-crystal Co_3O_4 nano-needles and their lithium storage properties. *J. Mater. Chem.* **2008**, *18*, 4397–4401.

[21] Lou, X. W.; Deng, D.; Lee, J. Y.; Feng, J.; Archer, L. A. Self-supported formation of needlelike Co_3O_4 nanotubes and their application as lithium-ion battery electrodes. *Adv. Mater.* **2008**, *20*, 258–262.

[22] Wang, D. S.; Ma, X. L.; Wang, Y. G.; Wang, L.; Wang, Z.Y.; Zheng, W.; He, X. M.; Li, J.; Peng, Q.; Li, Y. D. Shape control of CoO and $LiCoO_2$ nanocrystals. *Nano Res.* **2010**, *3*, 1–7.

[23] Li, Y. G.; Tan, B.; Wu, Y. Y. Mesoporous Co_3O_4 nanowire arrays for lithium ion batteries with high capacity and rate capability. *Nano Lett.* **2008**, *8*, 265–270.

[24] Li, Y. G.; Tan, B.; Wu, Y. Y. Freestanding mesoporous quasi-single-crystalline Co_3O_4 nanowire arrays. *J. Am. Chem. Soc.* **2006**, *128*, 14258–14259.

[25] Gao, Y. Y.; Chen, S. L.; Cao, D. X.; Wang, G. L.; Yin, J. L. Electrochemical capacitance of Co_3O_4 nanowire arrays supported on nickel foam. *J. Power Sources* **2010**, *195*, 1757–1760.

[26] Chan, C. K.; Peng, H. L.; Liu, G.; Mcilwrath, K.; Zhang, X. F.; Huggins, R. A.; Cui, Y. High performance lithium battery anodes using silicon nanowires. *Nat. Nanotechnol.* **2008**, *3*, 31–35.

[27] Ramana, C. V.; Zaghib, K.; Julien, C. M. Highly oriented growth of pulsed-laser deposited $LiNi_{0.8}Co_{0.2}O_2$ films for application in microbatteries. *Chem. Mater.* **2006**, *18*, 1397–1400.

[28] Li, Y. G.; Hasin, P.; Wu, Y. Y. $Ni_xCo_{3-x}O_4$ nanowire arrays for electrocatalytic oxygen evolution. *Adv. Mater.* **2010**, *22*, 1926–1929.

[29] Chen, G. Y.; Song, X. Y.; Richardson, T. J. Electron microscopy study of the $LiFePO_4$ to $FePO_4$ phase transition. *Electrochem Solid-State Lett.* **2006**, *9*, A295–A298.